geographical analysis

Geographical Analysis ISSN 0016-7363

Space–Time Geostatistics for Geography: A Case Study of Radiation Monitoring Across Parts of Germany

Gerard B. M. Heuvelink,[1] Daniel A. Griffith[2]

[1]Department of Environmental Sciences, Wageningen University, Wageningen, The Netherlands, [2]School of Economic, Political and Policy Sciences, The University of Texas at Dallas, Richardson, TX

Many branches within geography deal with variables that vary not only in space but also in time. Therefore, conventional geostatistics needs to be extended with methods that estimate and quantify spatiotemporal variation and use it in spatiotemporal interpolation and stochastic simulation. This article briefly summarizes the main concepts of space–time geostatistics. Kriging in space and time can be done in much the same way as it is in a purely spatial setting. The main difficulties are in defining a realistic stochastic model that is assumed to have generated data and in characterizing and estimating the space–time correlation of that model. This article uses a model-based geostatistical approach to characterize space–time variability. The space–time variable of interest is treated as a sum of independent stationary spatial, temporal, and spatiotemporal components, which leads to a sum-metric space–time variogram model. Methods are illustrated with a case study of space–time interpolation of monthly averages of detected background radiation for a 5-year period in four German states.

Introduction

Traditionally, geostatistics has dealt with static spatial variables. This focus is not surprising because geostatistics has its roots in mining, where target variables often are constant for time periods much smaller than the geologic time scale. However, over the past few decades, the usefulness of geostatistics has been demonstrated not only in mining and geology, but also in many other branches of geography and the earth sciences. Consequently, geostatistical modeling also needs to address variables that change in time as well as in space, such as terrestrial greenhouse gas emissions, surface water quality, spread of diseases, fish stocks, real estate value pricing, and political voting preferences. The extension of kriging and other

Correspondence: Gerard B. M. Heuvelink, Department of Environmental Sciences, Wageningen University, P.O. Box 47, 6700 AA Wageningen, The Netherlands
e-mail: gerard.heuvelink@wur.nl

Submitted: October 14, 2008. Revised version accepted: December 3, 2009.

geostatistical techniques to the space–time domain is not straightforward. Incorporating time is more than just adding a third (or fourth, if depth or height is the third) dimension, because the behavior of a variable over time differs from its behavior over space, and characteristics of the temporal processes that cause temporal variation are often known to some degree. If a statistical model characterizing the spatiotemporal behavior of a variable is to be of any value, it has to take into account differences between variation in space and in time. For example, over time, periodicity associated with daily or seasonal patterns is common, whereas in space, periodic variation is less common.

If the dynamic processes behind the space–time distribution of a target variable are reasonably well understood, the most compelling approach is to incorporate these explicitly into a process-based model, using a state–space approach (e.g., Huang and Cressie 1996; Hoeben and Troch 2000; Heemink, Verlaan, and Segers 2001; Bertino, Evensen, and Wackernagel 2003; Heuvelink et al. 2006). Here, the state equation describes explicitly how the state (i.e., key variables) of a system at a current point in time depends on that of the previous point in time. Measurements of a state together with process knowledge contained in its state equation can be used recursively to predict the state over time and space using a Kalman filter. Space–time Kalman filtering has important advantages over empirical space–time kriging described in this article, but sufficient knowledge must be available to quantify the dynamic evolution of the system under study and to define its state equation. When a space–time process satisfies a stochastic partial differential equation (PDE), then its space–time covariance structure also may be derived from a description of the physical process (e.g., Kolovos et al. 2004). For many systems, particularly in the social sciences, characterization of space–time variability by a state equation or PDE may be too ambitious. An empirical approach may be more appropriate in such cases. Accordingly, a space–time geostatistical model may be specified and its parameters estimated from observed data. Although not physically based, this model must appreciate the fundamental differences between spatial and temporal variation and must include these differences in its structure and parameterization (Kyriakidis and Journel 1999; Heuvelink and Webster 2001; Gneiting 2002; Gething et al. 2007).

This article begins with a brief review of the main approaches in space–time geostatistics. Most of these stem from the earth sciences. We show that kriging and stochastic simulation in space and time can be done in much the same way as they are in a purely spatial setting. The main difficulties are in defining a realistic stochastic model that is assumed to have generated given data and in characterizing and estimating the space–time correlation of that model. Several approaches exist to model space–time correlation statistically, many of which require advanced mathematical statistics. We provide a brief review but focus on one particular approach adapted from model-based geostatistics (Diggle and Ribeiro 2007). Here the starting point is not the space–time covariance function; instead, a stochastic model of the space–time variable of interest is postulated from which the space–time

covariance can be explicitly derived. The proposed model treats the space–time variable as a sum of a trend model plus independent stationary temporal, spatial, and anisotropic space–time components. The resulting space–time variogram and associated kriging formulations are applied to a space–time interpolation study of background radiation across four German states for a 5-year period.

Space–time kriging

Consider a variable $z = \{z(\mathbf{s}, t) | \mathbf{s} \in S, t \in T\}$ that varies within a spatial domain S and a time interval T. Let z be observed at n space–time points $(\mathbf{s}_i, t_i)$, $i = 1, \ldots, n$. These space–time observations may be a time series of observations at one or multiple spatial locations, a spatial network of observations collected at one or multiple points in time, any arbitrary set of space–time points, or combinations of these scenarios. Although the number of observations n may be very large, observing z at each and every combination of time and space is impossible. To obtain complete space–time coverage of z requires some form of interpolation. The objective then is to obtain a prediction of $z(\mathbf{s}_0, t_0)$ at a point $(\mathbf{s}_0, t_0)$ at which z was not observed, where $(\mathbf{s}_0, t_0)$ typically is associated with the nodes of a fine space–time grid. To do this, z is assumed to be a realization of a random function Z having a full statistical model, including its space–time dependence structure. Next, $z(\mathbf{s}_0, t_0)$ is predicted from the observations or simulated from its conditional distribution. Sometimes knowledge about the space–time dependence of Z itself is the goal of a study. For instance, quantified space–time statistical dependencies may be instructive for the exploration, comparison, interpretation, and explanation of the magnitude of temporal, spatial, and spatiotemporal variation and are essential prerequisites for optimizing spatiotemporal monitoring designs (De Gruijter et al. 2006; Brus and Heuvelink 2007).

The space–time variation of Z can be characterized by first decomposing it into a deterministic trend m and a zero-mean stochastic residual V as follows:

$$Z(\mathbf{s}, t) = m(\mathbf{s}, t) + V(\mathbf{s}, t) \tag{1}$$

The trend m is a deterministic, structural component representing large-scale variation. The residual is a stochastic component representing small-scale, noisy variation. Alternatively, the trend may be thought of as that part of Z that can be explained physically or empirically, using auxiliary information. The residual is the leftover part, which still holds information when it is correlated in space and/or time. The decomposition of Z into a trend and a residual is a subjective choice made by a modeler (Diggle and Ribeiro 2007). There is no unique way to decompose Z, and different modelers make different choices. Also, different decompositions may be made at various scales and for various levels of auxiliary information.

Characterization of a trend

As mentioned earlier, often the behavior of a variable over time is entirely different from its behavior over space. This difference can be represented in the trend of a space–time model specification. For instance, nitrous oxide emissions from agricultural and natural land are causally dependent on factors such as climate, vegetation type, atmospheric deposition, land management, and soil properties (Stehfest and Bouwman 2006). Ignoring these types of factors would be unwise when interpolating nitrous oxide emission measurements in space and time. Similarly, space–time modeling and estimation of black smoke particulate matter concentrations benefit from accounting for explanatory variables such as chimney density, distance to nearest industrial area, and land use (Fanshawe et al. 2008). Ideally, the trend would be a process-oriented, physical-deterministic model component that would lead to the state–space approach described previously and space–time Kalman filtering. However, when deterministic modeling is not feasible, due to a lack of understanding of the underlying governing processes or because external forces and boundary conditions governing the behavior of a target variable are unknown, one may rely on a regression-type model relating the dependent to the explanatory variables in an empirical way. The simplest approach, and the one used here, is to assume a trend that is a linear relationship between the (possibly transformed) dependent and explanatory variables, as in linear multiple regression.

After a trend has been specified and its parameters estimated, it may be subtracted from Z so that attention may be directed to the space–time stochastic residual V. With this approach, uncertainties in the detrending procedure are not taken into account in any subsequent analysis. In kriging, this drawback causes the interpolation uncertainty to appear smaller than it is. This problem can be avoided by accounting for uncertainties in the trend coefficients, such as is done in universal kriging (Diggle and Ribeiro 2007). The universal kriging approach is pursued in this article. Thus, the trend m can be written as

$$m(\mathbf{s}, t) = \sum_{i=1}^{p} \beta_i f_i(\mathbf{s}, t) \tag{2}$$

where the β_i are unknown regression coefficients, the f_i are predictors that must be known exhaustively over the space–time domain, and p is the number of predictors.

Characterization of the stochastic residual

Throughout this article, we assume that the zero-mean stochastic residual V is multivariate normally distributed. Given this assumption, the only information lacking is its autocovariance function,

$$C(\mathbf{s}_i, t_i, \mathbf{s}_j, t_j) = E[V(\mathbf{s}_i, t_i) \times V(\mathbf{s}_j, t_j)] \tag{3}$$

Alternatively, we may characterize the second-order properties of V with the variogram γ as follows:

$$\gamma(\mathbf{s}_i, t_i, \mathbf{s}_j, t_j) = \frac{1}{2}E[(V(\mathbf{s}_i, t_i) - V(\mathbf{s}_j, t_j))^2] \tag{4}$$

To facilitate the estimation of C (or γ) from observations, some limiting additional simplifying assumptions are necessary. This topic is addressed in the ''Modeling space–time variation'' section.

Space–time kriging and stochastic simulation

Once the trend and the covariance function of a residual term have been specified, (space–time) interpolation can be done in the usual way. Universal kriging yields the best linear unbiased predictor (with minimum expected mean squared error among all possible predictors under multivariate normality) of $Z(\mathbf{s}_0, t_0)$ as

$$\hat{z}(\mathbf{s}_0, t_0) = \mathbf{m}_0^T\ \hat{\beta} + \mathbf{c}_0^T\mathbf{C}_n^{-1}\left(\bar{\mathbf{z}} - \mathbf{M}\hat{\beta}\right) \tag{5}$$

(Bivand, Pebesma, and Gómez-Rubio 2008, section 8.5), where $\mathbf{M}$ is an $n \times p$ design matrix of predictor variables at the observation points, $\mathbf{m}_0$ is a vector of predictors at the prediction point, $\mathbf{C}_n$ is an $n \times n$ variance–covariance matrix for the n residuals at the observation points, $\mathbf{c}_0$ is a vector of covariances between the residuals at the observation and prediction points, and $\bar{\mathbf{z}}$ is a vector of observations $z(\mathbf{s}_i, t_i)$. The regression coefficients are estimated with $\hat{\beta}$ in the usual way, using generalized least squares.

The variance of the universal kriging prediction error is given by

$$\begin{aligned}\sigma^2(\mathbf{s}_0, t_0) &= \mathrm{var}(Z(\mathbf{s}_0, t_0) - \hat{Z}(\mathbf{s}_0, t_0)) \\ &= C(\mathbf{s}_0, t_0, \mathbf{s}_0, t_0) - \mathbf{c}_0^T\mathbf{C}_n^{-1}\mathbf{c}_0 \\ &\quad + (\mathbf{m}_0 - \mathbf{M}^T\mathbf{C}_n^{-1}\mathbf{c}_0)^T(\mathbf{M}^T\mathbf{C}_n^{-1}\mathbf{M})^{-1}(\mathbf{m}_0 - \mathbf{M}^T\mathbf{C}_n^{-1}\mathbf{c}_0)\end{aligned} \tag{6}$$

The universal kriging equations (5) and (6) remain basically the same, whether or not a temporal dimension is included. Thus, this perspective posits that spatiotemporal kriging and spatial kriging do not differ. However, one possible difference worth mentioning is that, in the space–time situation, predictions are often forecasts. When predictions into the future are based on observations in the past and present, space–time kriging becomes an extrapolator, instead of an interpolator, along the time axis. This feature has no effect on the kriging equations but does cause the predictions to become less accurate (i.e., larger kriging variance) because information comes from one direction only. When future observations are used to predict the present, although smaller kriging variances result, improper representation of a dynamic trend may cause artifacts, such as when soil water content predictions increase in anticipation of future rainfall events (e.g., Snepvangers, Heuvelink, and Huisman 2003).

Extending kriging to stochastic simulation and generating possible realities of Z (such as is needed in Monte Carlo uncertainty propagation analyses) is not difficult.

Existing algorithms, such as sequential Gaussian simulation, can be used (Goovaerts 1997; Bivand, Pebesma, and Gómez-Rubio 2008).

Modeling space–time variation

The main methodological difficulty with the application of space–time kriging lies in the characterization of the space–time covariance function. This function defines the covariance between the variable of interest at two space–time points, ($\mathbf{s}$, t) and ($\mathbf{s}+\mathbf{h}$, $t+u$), where $\mathbf{h}$ is the distance increment in space, and u is the increment in time. In the most general case, it is a function of $\mathbf{s}$, t, $\mathbf{h}$, and u, as in equation (3). However, this specification cannot be estimated because, in practice, we have observations of only one realization from which to infer a covariance function. The common solution to this problem is to introduce a stationarity assumption, which posits that the covariance of $V(\mathbf{s}, t)$ and $V(\mathbf{s}+\mathbf{h}, t+u)$ depends only on the distance in space $\mathbf{h}$ and distance in time u between the points: $C(\mathbf{s}, t, \mathbf{s}+\mathbf{h}, t+u) = C(\mathbf{h}, u)$. Although typically $\mathbf{h}$ is two dimensional, assuming isotropy in space means that Euclidean distance can be collapsed to one dimension in space, allowing both $\mathbf{h}$ and u to be treated as scalars, h and u.

The stationarity assumption greatly simplifies the space–time correlation structure of V, but a further practical simplification is needed to be able to estimate a space–time covariance function or variogram from a set of observations. Different approaches can be used, but one major difficulty is to ensure that the space–time covariance function is valid (i.e., positive definite; Gneiting 2002). Recently, many advanced methods have been published in the statistical literature to define classes of valid space–time covariance structures (e.g., Cressie and Huang 1999; Gneiting 2002; Kolovos et al. 2004; Stein 2005; Fuentes, Chen, and Davis 2008; Ma 2008; Mateu, Porcu, and Gregori 2008). A comprehensive review of these methods is beyond the scope of this article. The main distinction made is between separable and nonseparable space–time covariance functions. Separable covariance functions can be written as the product of a purely spatial and purely temporal component (Mateu, Porcu, and Gregori 2008). This allows efficient estimation and inference, but separability is restrictive and often requires unrealistic assumptions (Brown et al. 2001; Stein 2005; Fuentes, Chen, and Davis 2008). Therefore, attention has shifted to nonseparable space–time covariance structures, and recently many classes have been proposed, including structures that can handle anisotropies (Mateu, Porcu, and Gregori 2008) and negative covariances (Gregori et al. 2008). A comparison of different approaches also has been made (Huang et al. 2007).

Here we use a simpler approach and obtain a positive-definite nonseparable space–time covariance function with a model-based approach. We define a model for V and derive the associated covariance function from it. If each of the components of the model has a positive-definite covariance function, the positive definiteness of the space–time covariance function is guaranteed. In addition, a model-based formulation enhances interpretation of the space–time variability of

the underlying process because it makes the data-generation process explicit. We use the following model:

$$V(\mathbf{s}, t) = V_s(\mathbf{s}) + V_t(t) + V_{\text{st}}(\mathbf{s}, t) \tag{7}$$

where V_s is a purely spatial process (i.e., its realizations are constant over time), V_t is a purely temporal process (i.e., realizations are constant in space), and V_{st} is a space–time process for which distance in space is made comparable to distance in time by introducing a space–time anisotropy ratio. Introducing a norm, or ''metric,'' in space–time to compare distance in space with distance in time has been criticized because it ignores the fundamental difference between time and space (Myers 2002); nevertheless, it brings the analysis back to the familiar ground of three-dimensional geostatistical modeling. It also has a theoretical basis, because the metric space–time component can be shown to result from a space–time linear autoregressive model formulation and has a covariance function with an exponential shape (Griffith and Heuvelink 2009). All three components of equation (7) are assumed stationary and mutually independent, which leads to the ''sum-metric'' space–time covariance structure (Snepvangers, Heuvelink, and Huisman 2003):

$$C(h, u) = C_s(h) + C_t(u) + C_{st}\sqrt{h^2 + (\alpha \times u)^2} \tag{8}$$

The first two terms in the right-hand side of equation (8) allow for the presence of zonal anisotropies (i.e., variogram sills that are not the same in all directions). Zonal anisotropy occurs when the amount of variation in time is smaller or greater than that in space and/or that in joint space–time. The geometric anisotropy ratio α that appears in the third term in the right-hand side of equation (8) is needed because a unit of distance in space is not the same as a unit of distance in time. For instance, if $\alpha = 20$ m per day, then two points that are separated by 100 m in space and zero days in time have the same correlation as two points that are five days apart in time and zero meters in space, or as two points that are separated by 60 m in space and four days in time.

A case study

Most European countries established radiation monitoring networks as part of an emergency response system after the 1986 Chernobyl nuclear power plant accident. Among other things, networks provide information about detected gamma dose rates generated by gamma radiation. Data generally are recorded at 10-min intervals (De Cort and De Vries 1997). The primary purpose of radiation monitoring networks is to provide an emergency alert system capable of rapidly detecting large atmospheric releases of radiation. However, gamma dose rate data have potential utility in applications other than providing estimates of the radiation environment in cases of emergency. For example, aerosol concentrations data are very uncertain, and gamma dose rate data could be used to calibrate and improve climate models that examine the transport, transformation, and removal of these gases and aerosols.

Indeed, spatial variation in dose rates from gamma radiation can describe almost 60% of the spatial variation in radon gas (^{222}Rn) flux (Szevgary et al. 2007a; Szegvary, Leuenberger, and Conen 2007b). Time averages of gamma dose rates in non-emergency situations also provide delineations of background radiation caused by cosmic radiation, radioactive geological deposits, and normal anthropogenic nuclear activities, such as those that take place in nuclear power plants, hospitals, and research institutes (Melles et al. 2008). Maps portraying background radiation distributions are useful for improving detection efficiency in emergency situations (i.e., reduce false alarms).

We illustrate space–time geostatistics using monthly averaged gamma dose rates collected during a 5-year period, calendar years 2003–2007, for four German states (Niedersachsen, Nordrhein-Westfalen, Bremen, and Rheinland-Pfalz) in which 656 permanent gamma dose rate measurement devices are located (Fig. 1). Measurements were not made at all sites over the entire period; a total of 36,681 observations were

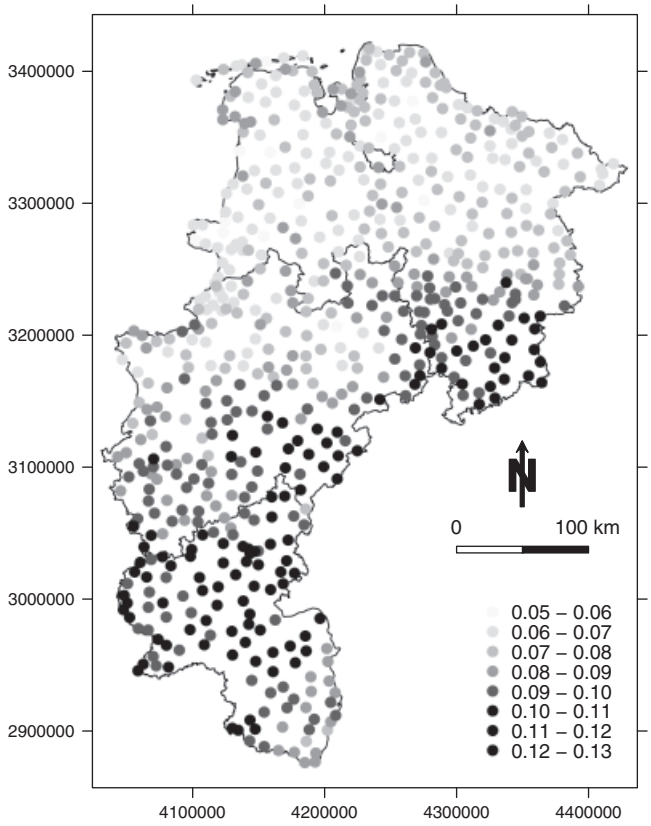

Figure 1. Study area with measurement locations. Grayscales are average gamma dose rates for month 1 (January 2003) in micro-Sieverts per hour. Coordinates are in the Lambert Equal Area, ETRS89 geodetic datum, GRS80 ellipsoid projection.

made. All geostatistical analyses were done using the R-gstat package (Bivand, Pebesma, and Gómez-Rubio 2008). Histograms of the data for arbitrarily selected months (1, 13, and 15) are given in Fig. 2. The histograms show that the data have a near-symmetric distribution and have no suspicious outliers. The same holds for all other months. Fig. 1 also portrays the spatial distribution of the data for month 1, which shows a north–south trend with larger values in the south. This trend probably is caused by differences in geology and elevation (the effect of cosmic radiation is greater at high altitudes), which can be taken into account by the trend of a space–time model. Here, we simply used a trend that is linear in latitude.

The experimental space–time variogram of the detrended data is given in Fig. 3. The marginal temporal and marginal spatial variograms are given in Fig. 4. An order of magnitude difference in variation in time and space exists. The spatial variation appears much greater than the temporal variation, even after removal of a spatial trend. There is a dip in the marginal temporal variogram at the 12-month time lag, indicating seasonal effects in gamma dose rates. As before, this pattern could be accounted for by examining the periodic temporal trend (which is not done here). A space–time variogram model was fitted to the data using a sum-metric model (i.e., equation [8]), where exponential functions were chosen for the temporal and spatiotemporal variograms, and the Bessel function was selected for the spatial component (Griffith and Layne 1999, pp. 146–52). Each of the three components has a nugget (c_0), partial sill (c_1), and range parameter (r). The spatiotemporal variogram has an additional anisotropy ratio α, resulting in 10 parameters in total. To speed up and improve convergence of the least squares iterative numerical fitting (Cressie 1985), the number of degrees of freedom for the model was reduced to three by imposing the following constraints, based on visual inspection of the experimental variogram:

(1) $c_0(\text{time}) + c_0(\text{space–time}) = 1.0\text{E} - 6$ (nugget of marginal temporal variogram);
(2) $c_0(\text{time}) + c_0(\text{space–time}) + c_1(\text{time}) + c_1(\text{space–time}) = 1.1\text{E} - 5$ (sill of marginal temporal variogram);
(3) $r(\text{time}) = 6$ months (temporal range parameter, effective range equals 18 months);
(4) $c_0(\text{space}) + c_0(\text{space–time}) = 2.0\text{E} - 5$ (nugget of marginal spatial variogram);
(5) $c_0(\text{space}) + c_0(\text{space–time}) + c_1(\text{space}) + c_1(\text{space–time}) = 1.6\text{E} - 4$ (sill of marginal spatial variogram);

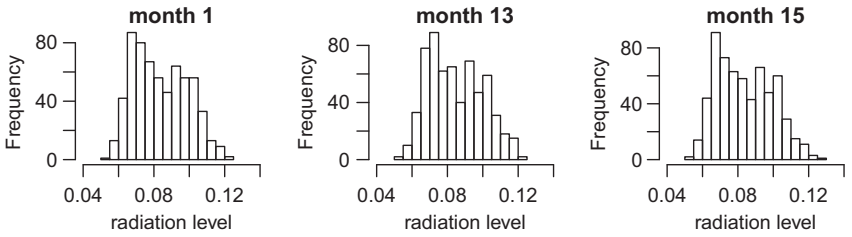

Figure 2. Histograms of gamma dose rate observations (μSv/h) for three arbitrary months.

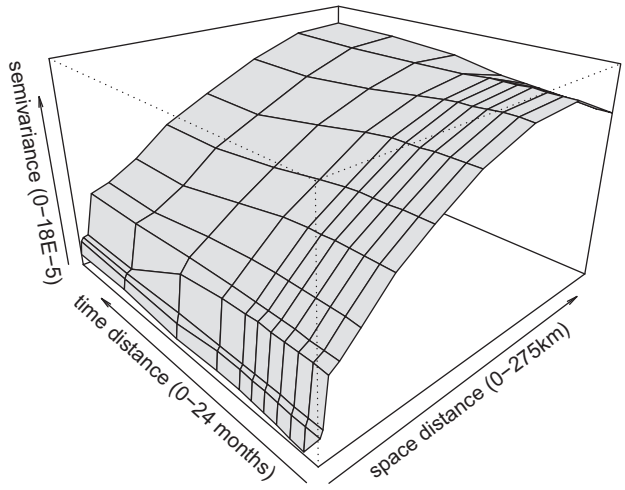

Figure 3. Perspective view of space–time experimental variogram.

(6) r(space) = 35 km (spatial range parameter, effective range equals 140 km); and,

(7) c_0(time) + c_0(space) + c_0(space–time) + c_1(time) + c_1(space) + c_1(space–time) = 1.63E − 4 (total sill).

The resulting parameter values are given in Table 1. The fitted model also is represented by solid lines superimposed on the marginal variograms in Fig. 4. Overall, the fit is satisfactory, although it might be improved by taking the seasonal trend into account. Also, the fitted marginal spatial variogram fails to incorporate the sudden increase for short lags. The variogram model was fitted to the entire space–time experimental variogram, which may be one reason why the fitting to the marginal experimental variograms may appear sub-optimal.

The majority of the total variation is accounted for by the spatial component, whereas the temporal and spatiotemporal components have a much smaller contribution. This result suggests that spatial patterns are stable over time and hardly change between months. Even though the temporal and spatiotemporal components are small relative to the spatial component, ignoring these would prevent any model variation in time, which is unrealistic (e.g., see observations plotted in Fig. 5). A space–time component V_{st} also is important to include, because complete space–time separation with only a spatial component V_s and a temporal component V_t implies that spatial patterns are identical at all time points and that temporal dynamics are the same everywhere, which is counter to evidence provided by the observations. Excluding a space–time component would also cause singularity problems, because many observations were taken from all four corners of space–

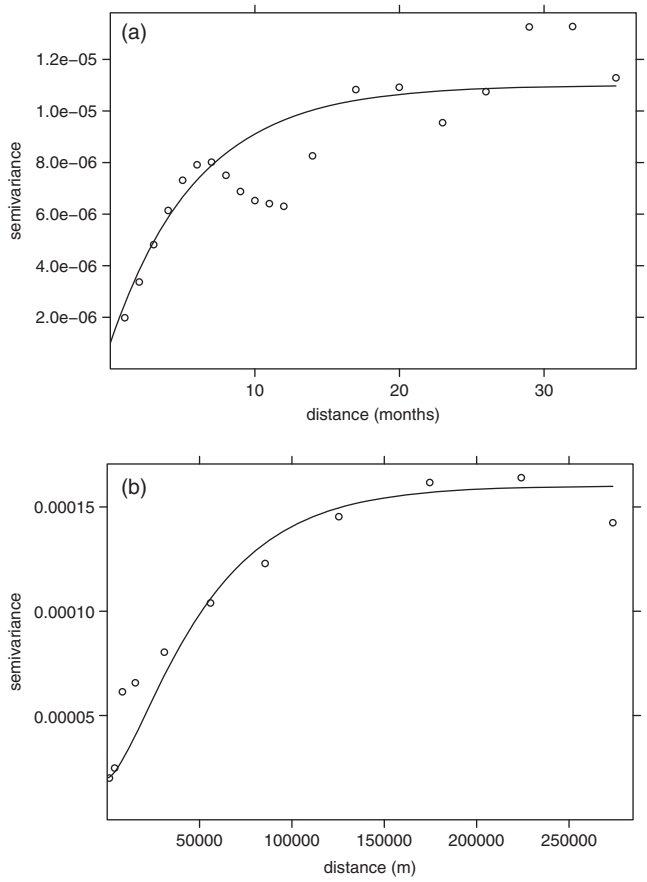

Figure 4. Marginal experimental variograms (dots) and fitted models (solid line): (a) temporal; (b) spatial.

time rectangles (Rouhani and Myers 1990; Snepvangers, Heuvelink, and Huisman 2003).

Now space–time kriging can be used to make predictions and quantify the prediction error at any space–time point using all of the data. Here we present results as time series near three arbitrarily chosen measurement locations (Fig. 5), three arbitrarily chosen nonmeasurement locations (Fig. 6), and in the form of maps

Table 1 Fitted Parameters of the Space–Time Variogram Model

c_0 (time)	c_1 (time)	r (time)	c_0 (space)	c_1 (space)	r (space)	c_0 (space –time)	c_1 (space –time)	r (space –time)	α
0	0.3E − 5	6 months	1.9E − 5	13.3E − 5	35 km	0.1E − 5	0.7E − 5	6 km	10 km/ month

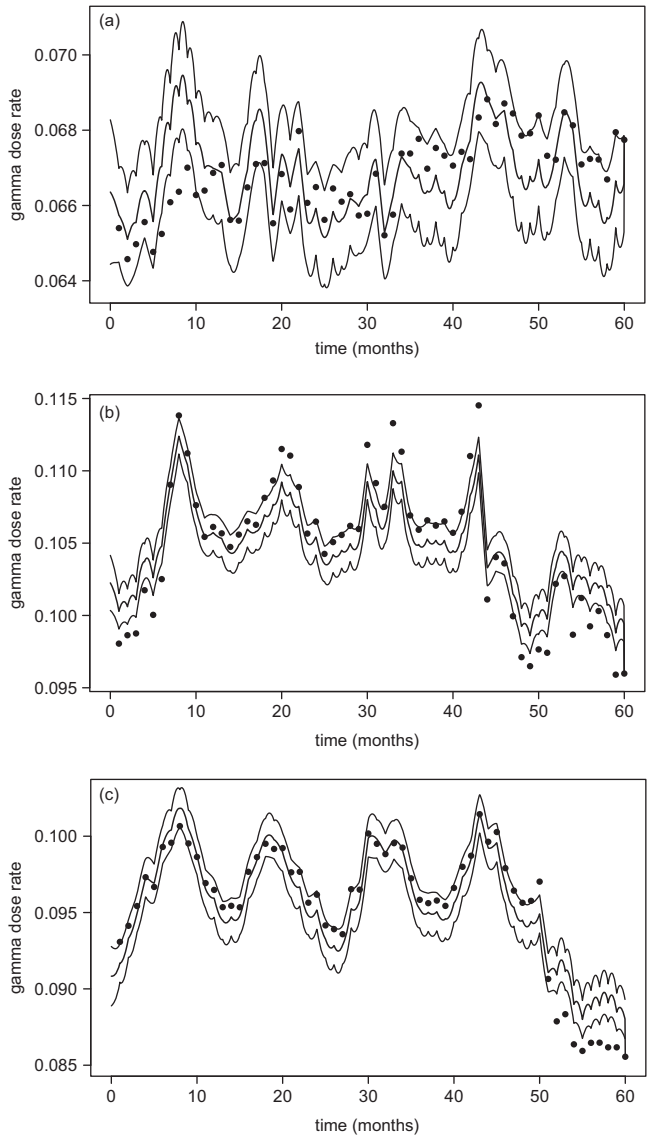

Figure 5. Kriging predictions over time in the immediate vicinity of three arbitrary measurement locations; thin lines are predictions ± one prediction error standard deviation. Dots are measurements. (a) $x = 4{,}184{,}364$, $y = 3{,}384{,}588$; (b) $x = 4{,}080{,}946$, $y = 3{,}101{,}289$; (c) $x = 4{,}143{,}018$, $y = 2{,}892{,}560$.

for two arbitrarily chosen time points (Fig. 7). To reduce computational complexity, the search radius of the kriging window was limited to a maximum of 700 closest observations (where ''closest'' is defined in terms of the degree of correlation). Although this number appears to be more than sufficient, in this case it may still be

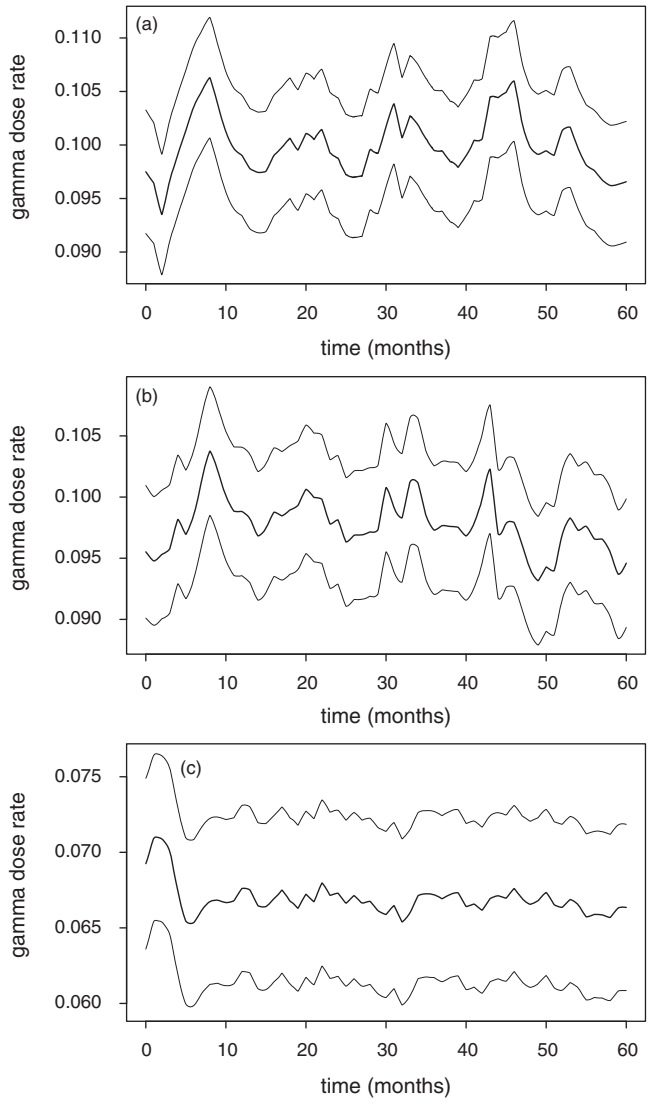

Figure 6. Kriging predictions over time at three arbitrary nonmeasurement locations; thin lines are predictions ± one prediction error standard deviation. (a) $x = 4{,}321{,}000$, $y = 3{,}210{,}000$; (b) $x = 4{,}075{,}412$, $y = 3{,}104{,}620$; (c) $x = 4{,}186{,}738$, $y = 3{,}323{,}123$.

too limited because of the many repeated measurements at each location (i.e., up to 60). However, using more observations would slow down the computations too much and may create numerical instabilities.

Fig. 5 shows that temporal patterns are similar for all three measurement locations, with small values in winter and large values in (late) summer. However,

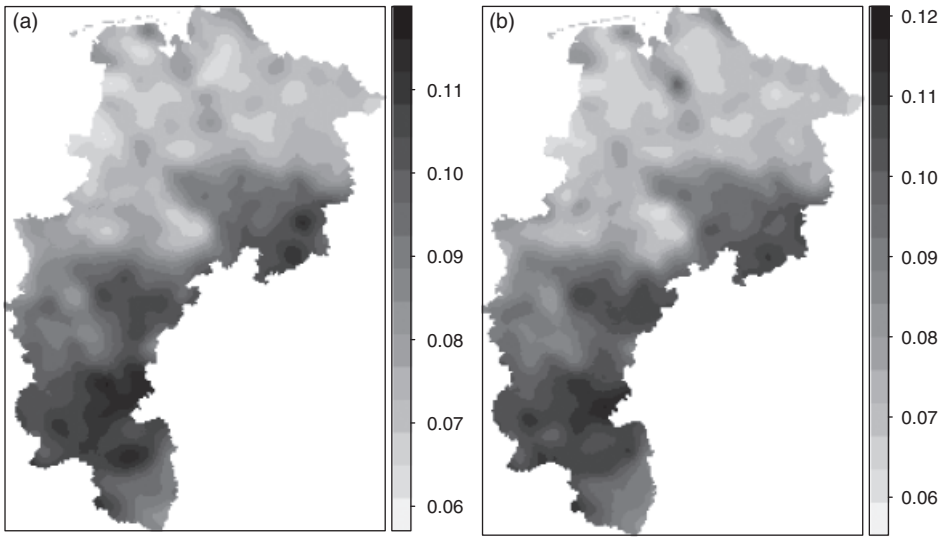

Figure 7. Kriging predictions over space at two arbitrary time points: (a) month 13; (b) month 51.

differences between stations are clear, particularly with respect to the mean value and the magnitude of variation. Predictions also can differ systematically from the measurements over longer time periods. For instance, predictions shown in Fig. 5a (first year) and Fig. 5c (final year) are greater than their corresponding observations. Apparently, neighboring stations have greater gamma dose rates, which are incorporated in the space–time kriging and cause a correction to greater values. Prediction intervals seem to represent the uncertainty adequately, because roughly two-thirds of the observations are contained within the prediction intervals. Fig. 6 shows that predictions at locations that are not close to an observation site are smoother than those near observation sites and that the seasonal effect is much less pronounced. Prediction intervals also are wider, and their width is practically constant over time. This finding is expected, because the main source of prediction error is spatial variability, which essentially does not change over time.

Fig. 7 confirms that the general spatial pattern of the gamma dose rate is persistent over time, with large values in the south and southeast and small values in the north. Differences between the two maps of predictions are very small. The maps of kriging standard deviations (Fig. 8) show that prediction errors are small (typically one order of magnitude smaller than the predicted values), with a spatial pattern that reflects the spatial configuration of the observation locations. Because the distribution of measurement locations is fairly uniform (see Fig. 1), the prediction error standard deviation is almost constant in the interior of the study area. The largest prediction errors are observed at the boundary of the area; however, the effect is not strong because a greater relative concentration of measurement loca-

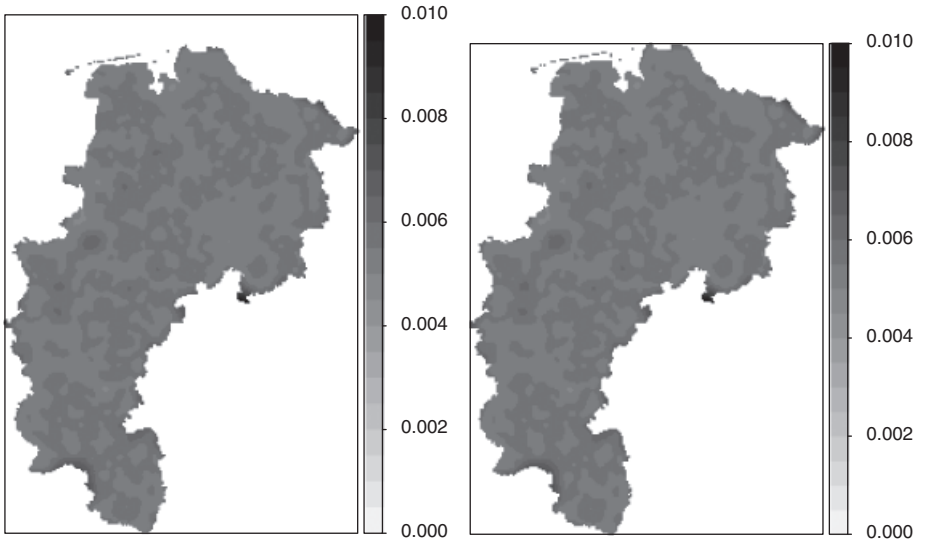

Figure 8. Kriging prediction error standard deviations over space at two arbitrary time points: (a) month 13; (b) month 51.

tions exists in the border areas (Fig. 1). Because the geostatistical model is dominated by the spatial component, the maps presented in Figs. 7 and 8 will not differ very much from maps obtained with conventional spatial kriging.

Discussion and conclusion

During the past few decades, interest in space–time geostatistics has grown, although applications are still restricted mainly to academic research. One of the obstacles to mainstream applications is the difficulty in building a space–time model, in particular, the space–time variogram. The space–time variogram should provide a realistic description of space–time variability and should not be too complex to be feasible to determine from available data. Development of general and flexible space–time covariance structures is an active research area within statistics, but more effort is needed to communicate results with geostatisticians and to embed results in geostatistical practice. Also, approaches that derive space–time covariance structures from explicit models of random functions assumed to have generated given data—be it space–time autoregressive moving average models or PDEs—deserve attention. These approaches are attractive because they express spatial and temporal relationships in a simple and natural way, with links to social and physical processes such as interaction, attraction, repulsion, diffusion, and convection (Whittle 1963; Bennett 1979; Griffith and Csillag 1993; Øksendal 2003; Kolovos et al. 2004). In practice, purely spatial or temporal processes also may be present, leading to a formulation that involves sums of temporal, spatial, and spatiotemporal components. An implicit assumption is that these components act

independently, which may not be realistic. Formulations that take into account interactions among these components may need to be developed and their associated variograms derived.

Constraints on variogram parameters in the empirical example presented here cause the overall fit to deteriorate but were imposed to ensure convergence to a near-global optimum of least-squares fitted parameters. Tools for fitting the space–time variogram to experimental variograms remain poorly developed. To date, fitting the parameters of the sum-metric model has been tried with ad hoc trial-and-error methods (Heuvelink, Musters, and Pebesma 1997) and by relying on numerical optimization techniques (Snepvangers, Heuvelink, and Huisman 2003). The extension from simple or ordinary to universal kriging may impose additional problems, namely, that least-squares solutions give biased results and suggest the use of restricted maximum likelihood techniques (Diggle and Ribeiro 2007; Marchant and Lark 2007).

The case study presented here involves predicting monthly averaged gamma dose rates for four German states over a 5-year period. The data show a dominant spatial component, which led us to conclude that spatial patterns of radiation are stable over the time period studied; this is confirmed by kriging. Temporal patterns are less consistent over space, although the seasonal effect is noticeable. Improved modeling that would incorporate a seasonal effect, geology, and elevation in the trend (Melles et al. 2008) would result in more realistic and more accurate predictions. However, even with a simple spatial trend model, observation density in space and time is sufficiently large to ensure that the resulting space–time coverage of gamma dose rate predictions has a small associated prediction error. The dominance of the spatial component suggests that an alternative, purely spatial model might represent the space–time distribution of the gamma dose rates as well as the space–time model used here. Likelihood-ratio tests comparing the spatial and spatiotemporal models may be used to analyze whether use of the more complex spatiotemporal model is worthwhile. This test result might reveal that, from a prediction error variance perspective, the spatiotemporal model provides no significant improvement over the purely spatial model. However, the spatial model would fail to represent the dynamic behavior of the gamma dose rates, for example, as presented in Fig. 5. Although the temporal variation is much smaller in magnitude than the spatial variation, it may be of specific interest to users concerned with temporal departures from the long-term background pattern. Likewise, the subtle differences in spatial patterns such as those presented in Fig. 7 may be valuable too, provided they are statistically significant.

Computationally, space–time kriging is more demanding than spatial kriging, because typically the number of observations is large as is the number of space–time prediction points. The total number of observations in our case study exceeds 36,000, which makes global kriging practically impossible. Instead, local search neighborhoods with 700 observations were used. This may have caused some artifacts in the prediction time series and maps.

The principal finding of this case study is that space–time geostatistics can produce large-scale space–time predictions of target variables and associated prediction errors. In doing so, it provides insight into the relative contribution of spatial, temporal, and spatiotemporal variation. This finding is not only useful for optimizing spatiotemporal sampling and monitoring designs but also provides insight into causes behind variation in space and time. Thus, space–time geostatistics contributes to the understanding and modeling of phenomena that vary in space and time.

Acknowledgements

We thank Ulrich Stoehlker and Sven Burbeck (Bundesamt für Strahlenschutz, Freiburg, Germany) for making the case study data available and for their valuable help with interpretations. We thank Edzer Pebesma (University of Münster, Germany) for tracing and removing a bug in R-gstat that caused the space–time kriging prediction to crash when a local search neighborhood was used. We thank anonymous reviewers for constructive remarks.

References

Bennett, R. J. (1979). *Spatial Time Series: Analysis—Forecasting—Control*. London: Pion.

Bertino, L., G. Evensen, and H. Wackernagel. (2003). ''Sequential Data Assimilation Techniques in Oceanography.'' *International Statistical Review* 71, 223–41.

Bivand, R. S., E. J. Pebesma, and V. Gómez-Rubio. (2008). *Applied Spatial Data Analysis with R*. New York: Springer.

Brown, P. E., P. J. Diggle, M. E. Lord, and P. C. Young. (2001). ''Space–Time Calibration of Radar Rainfall Data.'' *Journal of the Royal Statistical Society Series C—Applied Statistics* 50, 221–41.

Brus, D. J., and G. B. M. Heuvelink. (2007). ''Optimization of Sample Patterns for Universal Kriging of Environmental Variables.'' *Geoderma* 138, 86–95.

Cressie, N. (1985). ''Fitting Variogram Models by Weighted Least Squares.'' *Journal of the International Association of Mathematical Geology* 17, 563–86.

Cressie, N., and H. C. Huang. (1999). ''Classes of Nonseperable, Spatio-Temporal Stationary Covariance Functions.'' *Journal of the American Statistical Association* 94, 1–53.

De Cort, M., and G. De Vries. (1997). ''The European Union Radiological Data Exchange Platform (EURDEP): Two Years of International Data Exchange Experience.'' *Radiation Protection Dosimetry* 73, 17–20.

De Gruijter, J. J., D. J. Brus, M. F. P. Bierkens, and M. Knotters. (2006). *Sampling for Natural Resource Monitoring*. Berlin, Germany: Springer.

Diggle, P. J., and P. J. Ribeiro Jr. (2007). *Model-Based Geostatistics*. New York: Springer.

Fanshawe, T. R., P. J. Diggle, S. Rushton, R. Sanderson, P. W. W. Lurz, S. V. Glinianaia et al. (2008). ''Modelling Spatio-Temporal Variation in Exposure to Particulate Matter: A Two-Stage Approach.'' *Environmetrics* 19, 549–66.

Fuentes, M., L. Chen, and J. M. Davis. (2008). ''A Class of Nonseparable and Nonstationary Spatial Temporal Covariance Functions.'' *Environmetrics* 19, 487–507.

Gething, P. W., P. M. Atkinson, A. M. Noor, P. W. Gikandi, S. I. Hay, and M. S. Nixon. (2007). ''A Local Space–Time Kriging Approach Applied to a National Outpatient Malaria Data Set.'' *Computers and Geosciences* 33, 1337–50.

Gneiting, T. (2002). ''Nonseparable, Stationary Covariance Functions for Space–Time Data.'' *Journal of the American Statistical Association* 97, 590–600.

Goovaerts, P. (1997). *Geostatistics for Natural Resources Evaluation*. New York: Oxford University Press.

Gregori, P., E. Porcu, J. Mateu, and Z. Sasvári. (2008). ''On Potentially Negative Space Time Covariances Obtained as Sum of Products of Marginal Ones.'' *Annals of the Institute of Statistical Mathematics* 60, 865–82.

Griffith, D. A., and F. Csillag. (1993). ''Exploring Relationships Between Semi-Variogram and Spatial Autoregressive Models.'' *Papers in Regional Science* 72, 283–95.

Griffith, D. A., and G. B. M. Heuvelink. (2009). ''Deriving Space–time Variograms from Space–time Autoregressive (STAR) Model Specifications.'' Paper presented at the *StatGIS 2009* conference, Milos, Greece, June 17.

Griffith, D. A., and L. Layne. (1999). *A Case Book for Spatial Statistical Data Analysis*. New York: Oxford University Press.

Heemink, A. W., M. Verlaan, and A. J. Segers. (2001). ''Variance Reduced Ensemble Kalman Filtering.'' *Monthly Weather Review* 129, 1718–28.

Heuvelink, G. B. M., P. Musters, and E. J. Pebesma. (1997). ''Spatio-Temporal Kriging of Soil Water Content.'' In *Geostatistics Wollongong '96*, 1020–30, edited by E. Y. Baafi and N. A. Schofield. Dordrecht, The Netherlands: Kluwer.

Heuvelink, G. B. M., J. M. Schoorl, A. Veldkamp, and D. J. Pennock. (2006). ''Space–Time Kalman Filtering of Soil Redistribution.'' *Geoderma* 133, 124–37.

Heuvelink, G. B. M., and R. Webster. (2001). ''Modelling Soil Variation: Past, Present, and Future.'' *Geoderma* 100, 269–301.

Hoeben, R., and P. A. Troch. (2000). ''Assimilation of Active Microwave Observation Data for Soil Moisture Profile Estimation.'' *Water Resources Research* 36, 2805–19.

Huang, H.-C., and N. Cressie. (1996). ''Spatio-Temporal Prediction of Snow Water Equivalent Using the Kalman Filter.'' *Computational Statistics and Data Analysis* 22, 159–75.

Huang, H.-C., F. Martinez, J. Mateu, and F. Nontes. (2007). ''Model Comparison and Selection for Stationary Space–Time Models.'' *Computational Statistics and Data Analysis* 51, 4577–96.

Kolovos, A., G. Christakos, D. T. Hristopulos, and M. L. Serre. (2004). ''Methods for Generating Non-Separable Spatiotemporal Covariance Models with Potential Environmental Applications.'' *Advances in Water Resources* 27, 815–30.

Kyriakidis, P. C., and A. G. Journel. (1999). ''Geostatistical Space–Time Models: A Review.'' *Mathematical Geology* 31, 651–84.

Ma, C. S. (2008). ''Recent Developments on the Construction of Spatio-Temporal Covariance Models.'' *Stochastic Environmental Research and Risk Assessment* 22, S39–S47.

Marchant, B. P., and R. M. Lark. (2007). ''Robust Estimation of the Variogram by Residual Maximum Likelihood.'' *Geoderma* 140, 62–72.

Mateu, J., E. Porcu, and P. Gregori. (2008). ''Recent Advances to Model Anisotropic Space–Time Data.'' *Statistical Methods and Applications* 17, 209–23.

Melles, S. J., G. B. M. Heuvelink, C. J. W. Twenhöfel, and U. Stöhlker. (2008). ''Sampling Optimization Trade-Offs for Long-Term Monitoring of Gamma Dose Rates.'' In *ICCSA 2008, Part I, Lecture Notes in Computer Science*, Vol. 5072: 444–58, edited by O. Gervasi, B. Murgante, A. Laganà, D. Taniar, Y. Mun, and M. Gavrilova. Heidelberg, Germany: Springer.

Myers, D. E. (2002). ''Space–Time Correlation Models and Contaminant Plumes.'' *Environmetrics* 13, 535–54.

Øksendal, B. K. (2003). *Stochastic Differential Equations: An Introduction with Applications*. Berlin, Germany: Springer.

Rouhani, S., and D. E. Myers. (1990). ''Problems in Space–Time Kriging of Geohydrological Data.'' *Mathematical Geology* 22, 623–61.

Snepvangers, J. J. J. C., G. B. M. Heuvelink, and J. A. Huisman. (2003). ''Soil Water Content Interpolation Using Spatio-Temporal Kriging with External Drift.'' *Geoderma* 112, 253–71.

Stehfest, E., and L. Bouwman. (2006). ''N_2O and NO Emission from Agricultural Fields and Soils under Natural Vegetation: Summarizing Available Measurement Data and Modeling of Global Annual Emissions.'' *Nutrient Cycling in Agroecosystems* 7, 207–28.

Stein, M. (2005). ''Space–Time Covariance Functions.'' *Journal of the American Statistical Association* 100, 310–21.

Szevgary, T., F. Conen, U. Stohlker, G. Dubois, P. Bossew, and G. De Vries. (2007a). ''Mapping Terrestrial Gamma-Dose Rate in Europe Based on Routine Monitoring Data.'' *Radiation Measurements* 42, 1561–72.

Szegvary, T., M. C. Leuenberger, and F. Conen. (2007b). ''Predicting Terrestrial Rn-222 Flux Using Gamma Dose Rate as a Proxy.'' *Atmospheric Chemistry and Physics* 7, 2789–95.

Whittle, P. (1963). ''Stochastic Processes in Several Dimensions.'' *Bulletin of the International Statistical Institute* 40, 974–94.